Contents lists available at ScienceDirect

Physics Letters B

Production of Z'-boson resonances with large width at the LHC

E. Accomando [a], F. Coradeschi [b], T. Cridge [c], J. Fiaschi [d], F. Hautmann [e,f,g,h,*], S. Moretti [a], C. Shepherd-Themistocleous [i], C. Voisey [j]

[a] *School of Physics and Astronomy, University of Southampton, Highfield, Southampton SO17 1BJ, UK*
[b] *DAMTP, CMS, University of Cambridge, Wilberforce road, Cambridge, CB3 0WA, UK*
[c] *Department of Physics and Astronomy, University College London, WC1E 6BT, UK*
[d] *Institut für Theoretische Physik, Universität Münster, D 48149 Münster, Germany*
[e] *Elementaire Deeltjes Fysica, Universiteit Antwerpen, B 2020 Antwerpen, Belgium*
[f] *Theoretical Physics Department, University of Oxford, Oxford OX1 3NP, UK*
[g] *UPV/EHU University of the Basque Country, Bilbao 48080, Spain*
[h] *CERN, Theoretical Physics Department, CH 1211 Geneva, Switzerland*
[i] *Particle Physics Department, STFC, Rutherford Appleton Laboratory, Harwell Science and Innovation Campus, Didcot, Oxfordshire, OX11 0QX, UK*
[j] *Cavendish Laboratory, University of Cambridge, Cambridge CB3 0HE, UK*

ARTICLE INFO

ABSTRACT

Di-lepton searches for Beyond the Standard Model (BSM) Z' bosons that rely on the analysis of the Breit-Wigner (BW) line shape are appropriate in the case of narrow resonances, but likely not sufficient in scenarios featuring Z' states with large widths. Conversely, alternative experimental strategies applicable to wide Z' resonances are much more dependent than the default bump search analyses on the modelling of QCD higher-order corrections to the production processes, for both signal and background. For heavy Z' boson searches in the di-lepton channel at the CERN Large Hadron Collider (LHC), the transverse momentum q_T of the di-lepton system peaks at $q_T \lesssim 10^{-2} M_{ll}$, where M_{ll} is the di-lepton invariant mass. We exploit this to treat the QCD corrections by using the logarithmic resummation methods in M_{ll}/q_T to all orders in the strong coupling constant α_s. We carry out studies of Z' states with large width at the LHC by employing the program `reSolve`, which performs QCD transverse momentum resummation up to Next-to-Next-to-Leading Logarithmic (NNLL) accuracy. We consider two benchmark BSM scenarios, based on the Sequential Standard Model (SSM) and dubbed 'SSM wide' and 'SSM enhanced'. We present results for the shape and size of Z' boson signals at the differential level, mapped in both cross section (σ) and Forward-Backward Asymmetry (A_{FB}), and perform numerical investigations of the experimental sensitivity at the LHC Run 3 and High-Luminosity LHC (HL-LHC).

© 2020 The Author(s). Published by Elsevier B.V. This is an open access article under the CC BY license (http://creativecommons.org/licenses/by/4.0/). Funded by SCOAP³.

1. Introduction

The physics of Z' bosons has been extensively studied in the literature. For an exhaustive review, e.g., see Ref. [1]. There are numerous BSM scenarios in which the predicted Z' boson is characterised by a large width $\Gamma_{Z'}$. Examples of these include Techni-colour [2] and Composite Higgs Models [3–6], where additional Z' boson decay channels into exotic particles can take place. Model configurations also exist where the Z' boson generally couples to the first two generations and the third one differently [7,8]. It is notable that the couplings to the latter are not constrained by the most stringent Z' searches, i.e., those in Drell-Yan (DY) di-electron and di-muon channels [9–14]. Large $\Gamma_{Z'}/M_{Z'}$ values can result from such phenomena. A wide Z' resonance does not have an easily observable narrow BW line shape, instead it appears as a broad shoulder spreading over the SM background. In the above circumstances, the ratio $\Gamma_{Z'}/M_{Z'}$ can easily reach a magnitude of 50%, making a classical narrow BW line shape based analysis inappropriate.

Alternative experimental approaches can be applied to the case of a wide Z' resonance. Non-resonant searches, such as simply counting the number of events appearing above a certain lower

Table 1
Mass, width-to-mass ratio and couplings to fermions of the Z' boson in the SSM wide and SSM enhanced benchmark scenarios.

$U(1)'$	$M_{Z'}$ (GeV)	$\Gamma_{Z'}/M_{Z'}$	g'	g_V^u	g_A^u	g_V^d	g_A^d	g_V^e	g_A^e	g_V^ν	g_A^ν
$U(1)_{\text{SSMwide}}$	4500	10%	0.76	0.193	0.5	-0.347	-0.5	-0.0387	-0.5	0.5	0.5
$U(1)_{\text{SSMenhanced}}$	5000	27%	2.28	0.193	0.5	-0.347	-0.5	-0.0387	-0.5	0.5	0.5

threshold in the di-lepton invariant mass spectrum and comparing this measured value with the theoretical SM expectation, are for example performed. Another approach is to make use of additional observables supporting and/or complementing σ mapped in the di-lepton invariant mass M_{ll}. In this context, a simple observable that has been shown to be quite effective is A_{FB} [15–20].

Counting strategies rely heavily on the knowledge of the SM background in the large invariant mass region. Experiments generally use a combination of information from Monte Carlo (MC) simulation and data to estimate the SM background in the high-mass region of interest. An example approach is to parameterise a functional form using simulation and then constrain the overall amplitude using a low-mass control region assumed to be free from significant new physics content. This then provides a background estimate in the signal region of interest. The quality of this estimate will be subject to systematic uncertainties due to the theoretical understanding of the background, such as those due to Parton Distribution Functions (PDFs) or to missing higher order terms in theoretical calculations. As a result, having QCD corrections to the di-lepton spectrum well under control is of significant importance. Since A_{FB} is a ratio quantity some systematics will cancel and it is expected that QCD higher-order corrections will be lower than in the case of cross sections (and so their residual systematics). This was established to be the case for the PDF error in Ref. [16], in fact, to the extent that the differential A_{FB} in combination with the differential σ can even be used to improve PDF fits over a wide di-lepton invariant mass range of neutral DY final states [21–26]. As the shape of $d\sigma/dM_{ll}$ and dA_{FB}/dM_{ll} can change by factors that do not correspond to a trivial overall rescaling factor, one has to account for such QCD effects in the relevant experimental searches. In fact, it is of crucial importance to determine the impact of such corrections not only in these two differential distributions but also on the variables used for the selection of neutral DY events, i.e., the individual lepton transverse momentum (p_T^l) and pseudorapidity (η_l), as these may also be affected non-trivially.

This paper is motivated by the observation that, in the multi-TeV mass range of Z' boson searches, the transverse momentum q_T of the di-lepton system peaks at values much smaller than its invariant mass, $q_T \lesssim 10^{-2} M_{ll}$. We thus exploit the fact that the peaks in the q_T and M_{ll} distributions are two orders of magnitude apart to treat QCD higher-order corrections by using resummation techniques [27–36]. These techniques take into account logarithmically-enhanced contributions $\alpha_s^k \ln^n(M_{ll}/q_T)$ ($n \leq 2k$) to the differential cross section to all orders in α_s with NNLL accuracy, and neglect power suppressed contributions of order $\mathcal{O}(q_T/M_{ll})$. A number of computational tools implementing this method are available [37–55]. Currently, a benchmarking exercise based on these tools is being performed within the LHC Electroweak Working Group [56] in the context of precision DY studies in the SM. (Further information may be found in Ref. [57].) In this paper, we use the code reSolve described in [40], modified for our purposes to include the Z' boson contribution to the DY-channel in addition to the default SM ones (γ, Z).

The plan of this paper is as follows. In Sec. 2 we describe two illustrative theoretical frameworks embedding a Z' boson of significant width, which are called 'SSM wide' and 'SSM enhanced', where each is a variant of the SSM scenario [58]. In Sec. 3 we present the results, and give conclusions in Sec. 4.

2. Benchmark models

In this section, we introduce the benchmark models that we use to implement Z' resonances with large width. The model taken to be a reference model by the LHC experimental collaborations, ATLAS and CMS, when searching for wide Z' bosons, is the SSM [58] with the standard couplings given in [59]. We consider two variants of this model, which we call 'SSM wide' and 'SSM enhanced'.

In the SSM wide variant, the resonance width is increased by the opening of extra invisible decay channels. The chiral couplings to ordinary matter are unchanged with respect to the usual SSM model, while the resonance width is modified so as to have $\Gamma_{Z'}/M_{Z'} = 10\%$. In this scenario the resonance peak still has a BW line shape but it is broad enough to possibly escape detection via the standard bump hunt method. In the SSM enhanced case, a different mechanism is used and in this case the resonance width is enhanced by increasing the coupling between the Z' boson and the ordinary matter. We rescale the couplings by a factor of three with respect to the usual SSM model.

We set the model parameters so that the Z' resonance is beyond the current sensitivity of the ATLAS [60] and CMS [61,62] experiments at the LHC. In order to extract the bounds on the Z' boson mass and couplings, we use the computer codes of Refs. [16,63]. There, the significance of the BSM signal is estimated from the partonic cross section evaluated at Leading Order (LO) and convoluted with CT14NNLO PDF [64], with the addition of a mass dependent k-factor accounting for Next-to-LO (NLO) and Next-to-NLO (NNLO) QCD corrections [65,66] and acceptance as well as efficiency factors for both the di-electron and di-muon final states given in Ref. [67]. We then combine the significance for each of the two di-lepton channels to obtain the overall significance of the Z' resonance. In this way, we estimate the latest limits coming from the LHC Run 2 data analysis and set the benchmark model parameters accordingly.

Mass, width-to-mass ratio and couplings to the ordinary matter of the Z' boson within the two chosen benchmark scenarios are summarised in Table 1.

3. Numerical results

In this section, we show the results obtained by using the MC program reSolve [40], which performs the described transverse momentum resummation. This is a tool to compute differential distributions for colourless final states in hadron-hadron collisions, incorporating Born-level matrix element and QCD transverse momentum resummation [27–36] up to NNLL accuracy. The initial public version, reSolve-1.0 [40], focussed purely on the Standard Model, however for the benefit of this analysis it has been complemented with the addition of Z' boson production and decay, including interference with the SM γ, Z contribution. A complete description of the new version of the code will be given elsewhere [68]. Here, we just summarise the main features.

The resummed calculation implemented in reSolve is designed to take into account QCD higher-order logarithmic corrections of the type $\alpha_s^k \ln^n(M_{ll}/q_T)$, $n \leq 2k$, to the differential cross section $d\sigma/(dq_T dM_{ll} dY d\Omega)$ (where q_T, M_{ll} and Y are the di-lepton transverse momentum, invariant mass and pseudorapidity, while
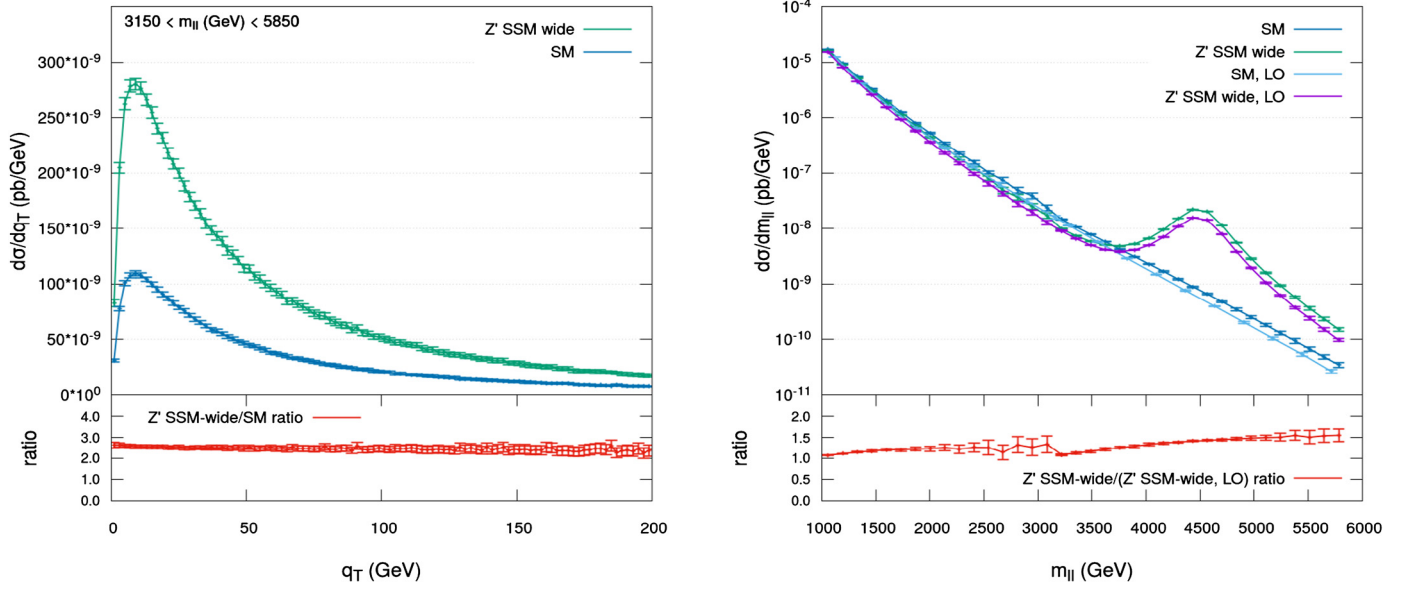
Fig. 1. (a) Distribution in the transverse momentum of the di-lepton system calculated at NNLL for the SM (dark blue) and the SSM wide (green) scenario with $M_{Z'} = 4.5$ TeV. We select the invariant mass region relevant for the Z' boson search 3150 GeV $\leq M_{ll} \leq$ 5850 GeV. The lower plot shows the ratio of the SSM wide Z' boson q_T spectrum to the SM one at NNLL. The bars indicate MC errors. (b) Di-lepton invariant mass (M_{ll}) distribution for the SM at LO (light blue) and NNLL (dark blue) and the SSM wide scenario at LO (purple) and at NNLL (green) with $M_{Z'} = 4.5$ TeV. The lower plot shows the ratio between the NNLL and LO invariant mass spectrum for the SSM wide case. The bars indicate MC errors.

Table 2
Acceptances in the SM and SSM wide scenario for kinematical cuts in the transverse momentum and pseudorapidity of the single leptons. The mass window 3150 GeV $\leq M_{ll} \leq$ 5850 GeV is selected. Here, the label 1(2) refers to the highest (lowest) transverse momentum lepton.

$U(1)'$	$p_T^1, p_T^2 \geq 20$ GeV	$\eta_1, \eta_2 \leq 2.5$	$p_T^1, p_T^2 \geq 20$ GeV; $\eta_1, \eta_2 \leq 2.5$
$U(1)_{\mathrm{SM}}$	0.99	0.95	0.95
$U(1)_{\mathrm{SSMwide}}$	0.99	0.96	0.96

Ω represents any additional variables internal to the final state that may be needed to fully define its phase space) up to NNLL for any k, by neglecting power-suppressed contributions of order $\mathcal{O}(q_T/M_{ll})$ at each order $k \geq 1$. The use of this tool for the calculations that follow is motivated by the fact that our search window is in the large invariant mass region, $M_{ll} \geq 3$ TeV, while the di-lepton transverse momentum distribution peaks around $q_T \sim \mathcal{O}(10$ GeV). The contributions from the non-logarithmic high-q_T tail of the distribution are thus expected to be power-suppressed in the Z' relative to the SM case. Given that the transverse momentum spectrum is strongly peaked at low transverse momenta, the approximation adopted should account for the majority of the contributions to the total cross section.

In Fig. 1a, we show the distribution in the transverse momentum of the di-lepton system for the SM and the SSM wide scenario with $M_{Z'} = 4.5$ TeV. We select the invariant masses in the range 3150 GeV $\leq M_{ll} \leq$ 5850 GeV, which corresponds to the search window $M_{Z'} - 3\Gamma_{Z'} \leq M_{ll} \leq M_{Z'} + 3\Gamma_{Z'}$ relevant to our studies. Clearly, the presence of the hypothetical Z' boson causes a relatively uniform increase in the q_T spectrum of about a factor of 3, compared to the SM values, at least in the low transverse momentum part dominated by the resummed contributions. Similar effects are seen for the SSM enhanced scenario. This is a pure NNLL prediction. The error bars shown in the plot are the MC errors. The statistical significance of the q_T distribution will be discussed later for the two benchmark models, separately. Here, we just highlight the introductory features coming from the NNLL calculation, as compared to the Born result. In Fig. 1b, we show the effect of the resummation on the di-lepton invariant mass spectrum in the SSM wide scenario with the same mass as before, $M_{Z'} = 4.5$ TeV. Here, we

see that higher-order corrections monotonically increase the differential cross section, moving from low to high invariant masses, reaching a roughly 50% magnitude at the right end of the spectrum.

Next, we consider the effect of a possible Z' boson on the acceptance by examining the distributions in the transverse momentum and pseudorapidity of the individual leptons detected, at the NNLL order. As before, we compare the SSM wide scenario with a representative Z' boson mass $M_{Z'} = 4.5$ TeV to the SM results. The presence of a wide Z' boson produces a larger differential cross section across all points in both differential cross sections, as expected. In particular, the ratio BSM/SM has a major increase at large absolute values of the lepton pseudorapidity and at the Jacobian peak of the lepton transverse momentum distribution. The acceptance however is not sensitive to higher-order corrections. Table 2 summarises the acceptance in transverse momentum and pseudorapidity of the individual leptons in the final state.

Then, we consider the discovery potential of the LHC for the wide Z' boson predicted by the SSM wide and SSM enhanced scenarios, by employing two different techniques: the invariant mass event counting and the associated measurements of the spectrum and of three other support variables, i.e., A_{FB}, the minimum transverse momentum of a single lepton, p_T^{min}, and the transverse momentum of the di-lepton system, q_T. For these calculations, a 9-point scale variation was performed in `reSolve` varying the renormalisation and factorisation scales by a factor of 2 around their default values and also, independently of this, varying the resummation scale by a factor of 2 up and down. As a result, we found that the scale dependence is negligible in comparison to the
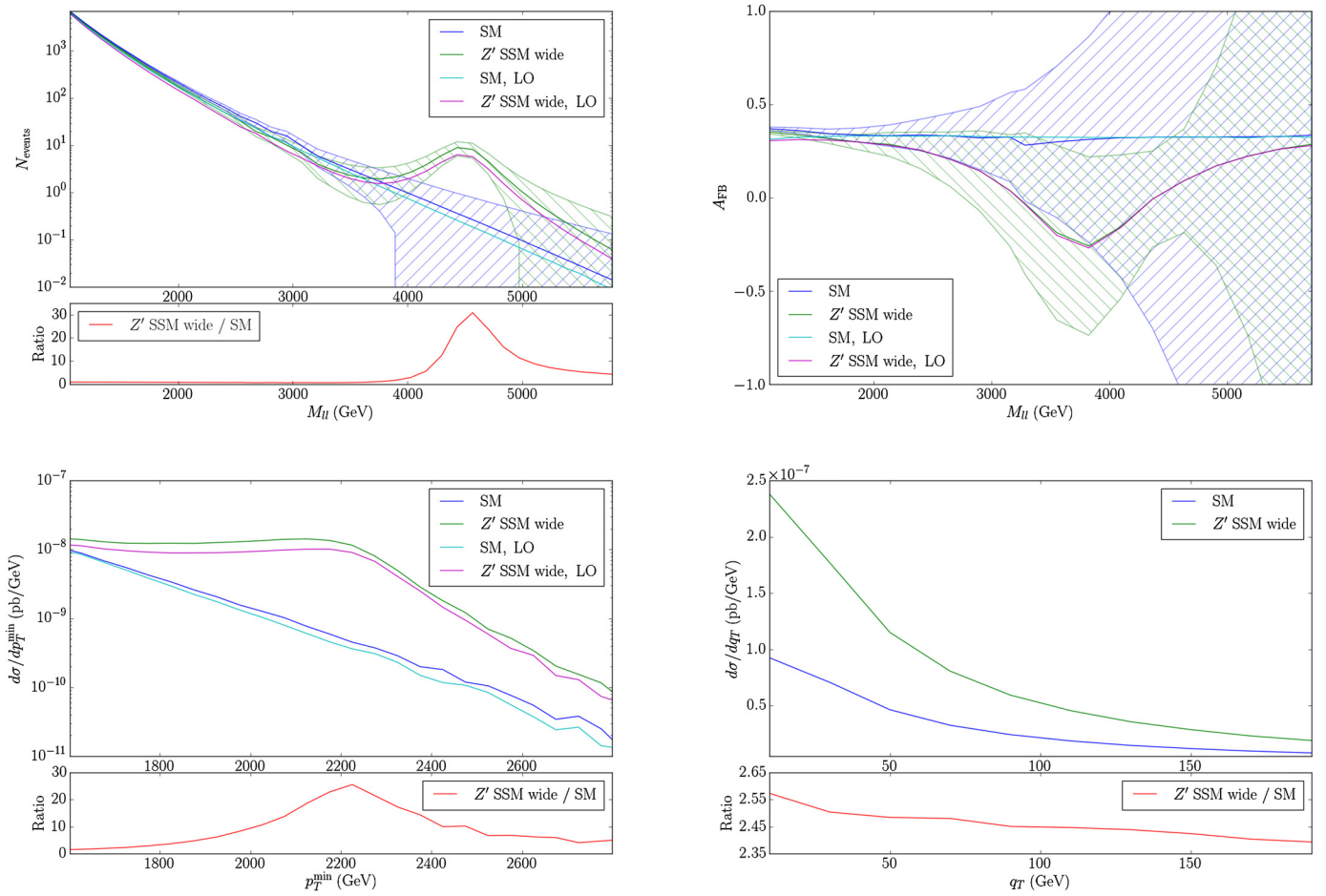
Fig. 2. (a) Number of events versus the di-lepton invariant mass within the SM and the SSM wide scenario with $M_{Z'} = 4.5$ TeV. We assume an integrated luminosity $L = 3000$ fb^{-1}. The results are calculated at Born and NNLL order, along with the statistical error (dominant). The BSM/SM ratio is presented in the sub-plot. (b) Same as above for A_{FB} as a function of the di-lepton invariant mass. (c) Distribution in the minimum transverse momentum of a single lepton within the SM and the SSM wide scenario with $M_{Z'} = 4.5$ TeV, computed at the LO and NNLL order. The BSM/SM ratio is presented in the sub-plot. We select the invariant mass window 3150 GeV $\leq M_{ll} \leq$ 5850 GeV. (d) Same as in (c) for the distribution in the transverse momentum of the di-lepton system at NNLL. For all plots, acceptance cuts are applied (see fourth column in Table 2).

statistical errors for the cases we consider. We therefore omit its error band, as well as the MC errors (indeed sub-dominant), in the upcoming figures. Statistical error bands only are shown and only for the NNLL cases.

We first discuss the SSM wide scenario. For this case, we consider an integrated luminosity of 3000 fb^{-1} corresponding to the HL-LHC. Fig. 2a presents the number of events versus the di-lepton invariant mass within the SM and the SSM wide scenario, calculated at both LO and NNLL. The error bands are purely statistical, as they completely dominate over the MC errors from our calculation with reSolve and over the scale dependence. The Z' resonance peak at $M_{Z'} = 4.5$ TeV is clear and outside of the statistical errors, indicating that this model could be detected at the HL-LHC through the di-lepton event counting analysis.

A_{FB} for the same scenario is presented in Fig. 2b. As before, we show both the SM and the SSM wide scenario at LO and NNLL order. The large error bands represent the statistical uncertainty on the A_{FB} as calculated according to [17]. The stability of the A_{FB} to the higher orders is demonstrated, while the complementarity of the A_{FB} to the invariant mass spectrum is also clear, with the A_{FB} in the SSM wide scenario deviating from the SM at lower invariant masses and peaking well before the Z' boson on-shell mass, $M_{Z'} = 4.5$ TeV. However, in this case the larger statistical uncertainty associated with A_{FB} suggests that the event counting analysis would offer greater promise. Any evidence in this spectrum could be made stronger by the additional measurement of

the minimum transverse momentum of a single lepton, p_T^{min}, and the di-lepton transverse momentum, q_T, given in Figs. 2c and 2d.

We then analyse the SSM enhanced model. For this case, we assume an integrated luminosity $L = 300$ fb^{-1} corresponding to the value expected at the LHC Run 3. Fig. 3a displays in the main plot the invariant mass spectrum for the SSM enhanced scenario with $M_{Z'} = 5$ TeV compared to the SM. We plot both the LO and NNLL results. The QCD corrections increase with the di-lepton invariant mass, reaching a 50% magnitude over the LO result at the Z' boson peak. The statistical uncertainties are represented by the error bands on the NNLL results. The presence of a wide Z' boson in this case causes a "shoulder" in the invariant mass spectrum beginning at around 3 TeV and continuing beyond 5 TeV. The potential excess of events as compared to the SM background is clearly evidenced in the BSM/SM ratio presented in the sub-plot, where the value of the ratio raises from 50 to 400 in the 4000 GeV $\leq M_{ll} \leq$ 5000 GeV mass window. However, in reality, for the projected luminosity at the LHC Run 3 the total number of events that one could count starting from a lower invariant mass threshold of 3 TeV is fairly small. On top of that, the width is so large that no discernible structure assignable to a Z' may exist in the cross section mapped in the invariant mass of the di-lepton pair. Due to the extreme lack of statistics and of any truly observable resonant peaking structure, no strong claim could then be made on the existence of new physics. We therefore consider other possible observables that may have distinctive trends that are significantly different from SM ex-
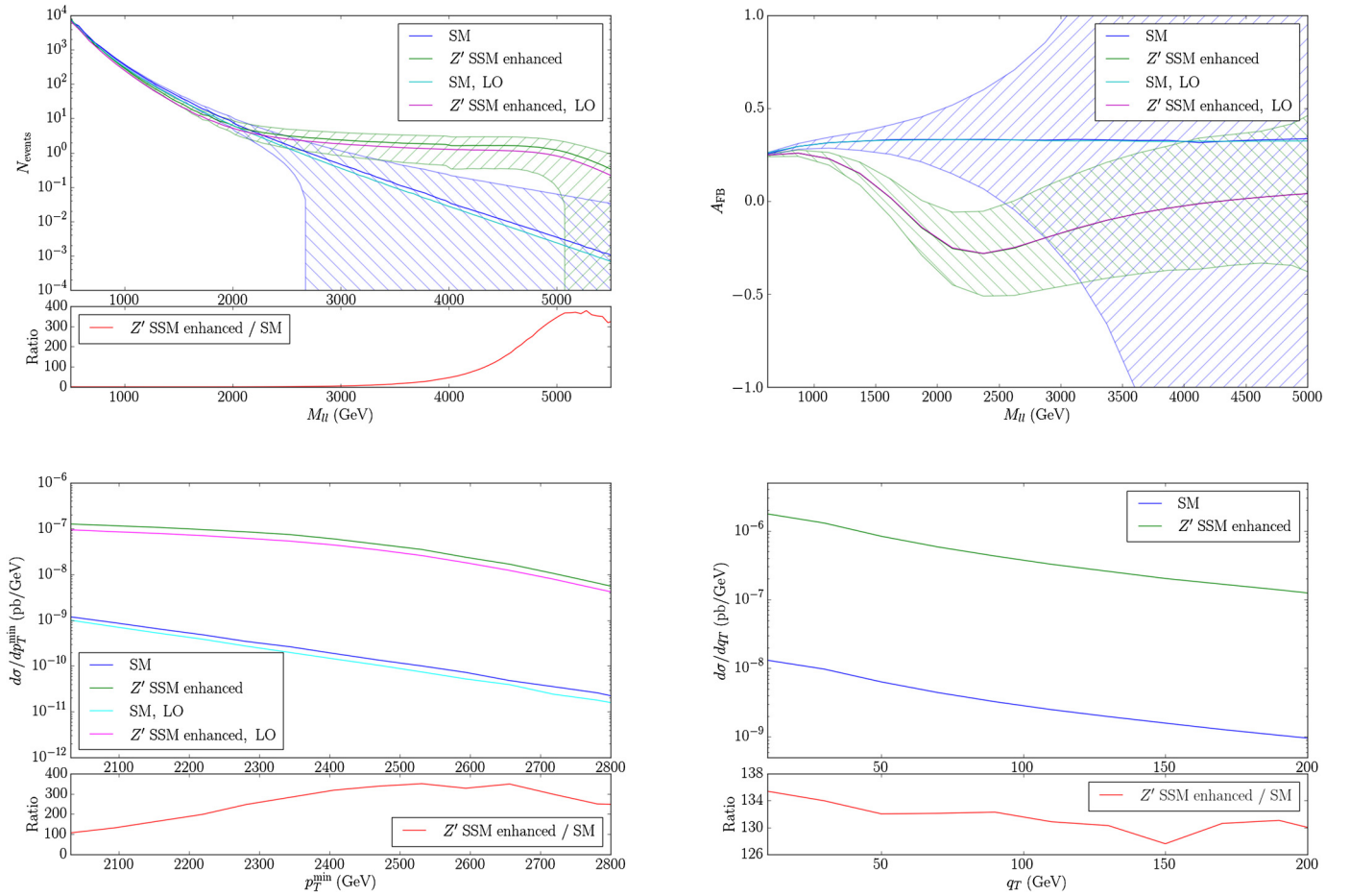
Fig. 3. (a) Number of events versus the di-lepton invariant mass within the SM and the SSM enhanced scenario with $M_{Z'} = 5$ TeV. We assume an integrated luminosity $L = 300$ fb^{-1}. The results are calculated at the LO and NNLL orders, along with the statistical error (dominant) on the NNLL results. The BSM/SM ratio is presented in the sub-plot. (b) Same as above for A_{FB} as a function of the di-lepton invariant mass. (c) Differential cross section in the minimum transverse momentum of a single lepton within the SM and the SSM enhanced scenario with $M_{Z'} = 5$ TeV, computed at the LO and NNLL orders. The BSM/SM ratio is presented in the sub-plot. We select the invariant mass window 4000 GeV $\leq M_{ll} \leq 6000$ GeV. (d) Same as (c) for the distribution in the transverse momentum of the di-lepton system. For all plots, acceptance cuts are applied (see fourth column in Table 2).

pectations, which may be exploited to establish a signal in neutral DY final states. For a wide Z' boson, interference effects between the BSM signal and SM background in such channels are significant. This implies two key aspects of the associated phenomenology. Firstly, unlike in the case of a narrow resonance where the BW peak position, giving the Z' boson mass, can readily be identified in a model-independent way, the broad structure in the $d\sigma/dM_{ll}$ distribution can no longer be optimally sought by assuming a narrow resonance signal structure. Secondly, other spectra such as dA_{FB}/dM_{ll}, $d\sigma/dp_T^{min}$ or $d\sigma/dq_T$ may show the aforementioned distinctive features away from the Z' peak itself, including in the low invariant mass tail where one would naively expect the SM to dominate. While it becomes impossible to design a model independent experimental search giving the best possible sensitivity in all cases, it conversely becomes possible to readily identify the underlying theoretical BSM scenario in presence of a signal.

We first consider A_{FB}, which has the advantage that it is constructed from a ratio of cross sections ($d\sigma/dM_{ll}$) and hence benefits from the cancellation of both experimental and theoretical systematic effects, as already intimated. Conversely, the statistical error is much larger for A_{FB} than it is for $d\sigma/dM_{ll}$. Hence, the relative advantages of these observables depends on the amount of integrated luminosity available at the LHC. Fig. 3b shows the A_{FB} observable in the SSM enhanced scenario. Once more the experimental statistical error bands dominate over the theoretical sources given by MC errors and scale dependence. The latter are

therefore not shown. Again both the stability of the A_{FB} observable with respect to higher orders and its complementarity to the invariant mass spectrum are clear. For the forward-backward asymmetry the Z' boson contribution, in fact, deviates from SM expectations at a level greater than the expected experimental statistical errors at invariant masses much lower than those where the "shoulder" starts to emerge over the SM di-lepton mass spectrum. Here, considering the region just above $M_{ll} \geq 1$ TeV where the A_{FB} starts showing the effect of the presence of a Z' boson, the number of events is much larger than in the region in the mass spectrum where departures from the SM expectation are observable, having of order one thousand events. Moreover, the A_{FB} shows a very well defined structure that significantly deviates from the SM yield. In the case of such a wide Z' boson, the measurement of A_{FB} could be decisive for a discovery.

Nonetheless, given its large width, the Breit-Wigner constant width approximation for the Z' resonances may no longer hold [69–73]. We therefore investigate next whether the behaviour we have described persists in the case of a more general running ("variable") width. To do this, we follow the treatment described in [74] and widely used at LEP, whereby $m_{Z'}\Gamma_{m_{Z'}}$ is replaced by $\hat{s}\Gamma_{m_{Z'}}/m_{Z'}$. In this case the running width term in the denominator of the propagator is smaller than the corresponding part for the standard constant width treatment before the resonance (as $\hat{s}/m < 1$), whilst it exceeds it after the resonance (as $\hat{s}/m > 1$). This then correspondingly increases (resp. decreases) the cross-section
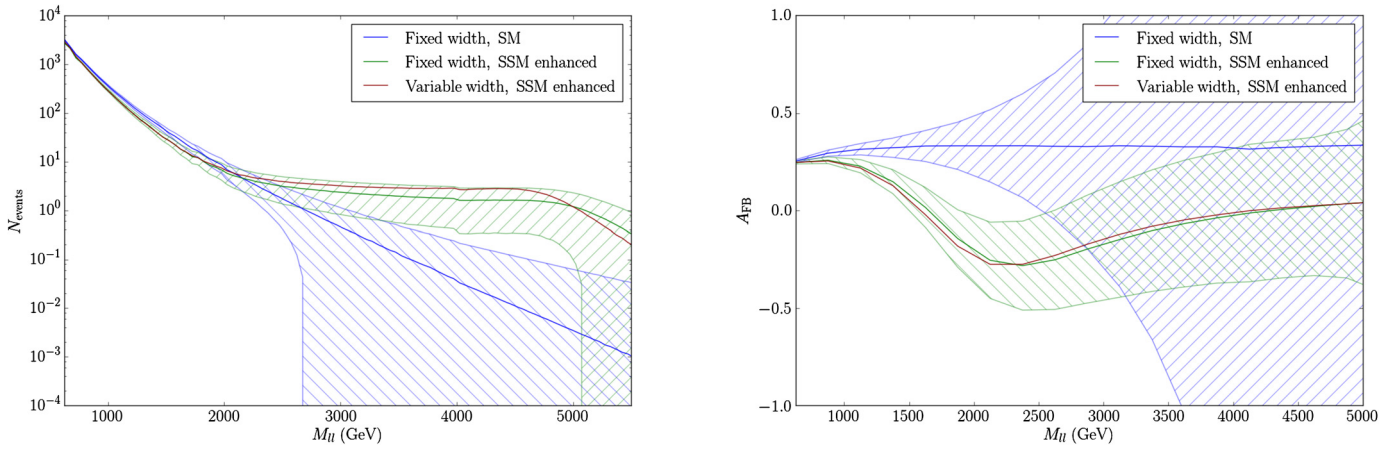
Fig. 4. (a) Number of events versus the di-lepton invariant mass within the SM and the SSM enhanced scenario with $M_{Z'} = 5$ TeV, comparing the fixed width (Breit-Wigner) and variable width schemes for the Z'. We assume an integrated luminosity $L = 300$ fb^{-1}. The results are calculated at NNLL and the statistical error (dominant) on the NNLL results is shown by the bands. (b) Same as above for A_{FB} as a function of the di-lepton invariant mass, again comparing the fixed width and variable width schemes for the Z'.

contributions from the Z' relative to the fixed-width case before (resp. after) the resonance. This will in general impact the overall cross-section and forward-backward asymmetry resonance and interference structure. One may expect A_{FB} to be less affected given that it is a ratio. Figs. 4(a) and 4(b) show variable-width results for the cross section and forward-backward asymmetry, respectively, in the SSM enhanced scenario. For the cross section in Fig. 4(a) the expected increase before the resonance and reduction after the resonance is observed. Nevertheless the effect is within the statistical error bands, and in fact slightly enhances the "shoulder" in the cross section. For the A_{FB} in Fig. 4(b) the effect is smaller still, as might be expected, and is well within the statistical errors, so that it does not change our analysis. It is worth noting that in the invariant mass range $M_{ll} \leq 2500$ GeV in Fig. 4(b) the pure Z' contribution to the cross section as well as its interference contribution both increase in magnitude, and the negative interference contribution of the Z' drives the forward-backward asymmetry negative sooner than in the fixed-width case, while in the invariant mass range (2500 GeV $\leq M_{ll} \leq 5000$ GeV) the positive pure Z' cross-section contribution is slightly enhanced, resulting in a very mildly increased A_{FB}. In fact this marginal change in the A_{FB} actually slightly enhances its shape, moving it away from the SM, albeit very slightly and well within the statistical errors. Finally we note that, as expected, both the cross section and forward-backward asymmetry are identical in the variable-width and fixed-width cases at the Z' resonance. In summary, the results for the cross section and A_{FB} and their consequent complementary benefits in searching for such a large width Z' signal are independent of the precise form of the partial width we assumed, with the changes due to variable width remaining within the statistical error bands and with the forward-backward asymmetry being particularly robust.

To support any preliminary evidence, one can consider other observables to tackle the search. One could consider the distribution in the minimum transverse momentum of a single lepton, p_T^{min}, as shown in Fig. 3c. Here we observe the relic of the Jacobian peak, flattened by the fact that the Z' boson is quite wide in this model. This peak is however more pronounced than the deviation in the falling cross section of the di-lepton mass spectrum, thus potentially helping to estimate the mass $M_{Z'}$. A third variable of interest is the differential cross section in the transverse momentum of the di-lepton pair, q_T. We see that in a search window around the Z' boson mass, 4000 GeV $\leq M_{ll} \leq 6000$ GeV shown in Fig. 3d, the q_T distribution is enhanced by the presence of the hypothetical Z' boson by a factor of one hundred or more compared

to the SM background. This effect is concentrated in the low q_T range, as expected (see also Fig. 1a), and is statistically significant. The measurement of q_T could therefore support the observation of an excess of events (a few) in the di-lepton spectrum and of a deviation (sizeable) in the shape of the A_{FB}, strengthening the experimental evidence in the event of the presence of new physics.

In addition to the excess of events predicted in both scenarios, either around the Z' resonance peak for the SSM wide case or spread over the shoulder for the SSM enhanced model, we also see a depletion of events at lower invariant masses due to the interference of the Z' boson contribution with the SM γ, Z one. This is shown in Figs. 2a and 3a, however it is unclear due to the larger ranges and so we show zoomed-in versions focusing on the lower invariant mass portions in Fig. 5. In both scenarios the depletion of events in the Z' case relative to the SM is statistically significant over at least part of this range. In the SSM enhanced case of Fig. 5b this effect is greater and extends over a wider invariant mass range and so is more promising. In this case a depletion of about 20% of the events for the SSM enhanced scenario considered could in principle be observed in the 1000 GeV $\leq M_{ll} \leq 1500$ GeV mass window. In conjunction with the shape difference seen at relatively low invariant masses in the A_{FB}, these effects at considerably lower invariant masses than the resonance peak may offer a further means of probing Z' physics.

4. Conclusions

The A_{FB} observable in Z' physics, other than being a time-honoured diagnostic probe, has recently been established to also be a discovery tool at the LHC whenever the new neutral massive gauge boson is wide, i.e., it displays a large ratio between its width $\Gamma_{Z'}$ and mass $M_{Z'}$. The advantages in this respect are twofold. Firstly, A_{FB} may reveal experimentally non-trivial structures in the invariant mass even when the cross section loses altogether its striking BW appearance. Secondly, it is much more stable than the latter in relation to systematic uncertainties from both the experimental and theoretical side, owing to A_{FB} being a ratio of cross sections. The first feature has been proven to be true quantitatively for a variety of Z' models whereas the second one has recently been demonstrated for the case of the PDF error. Herein, we have complemented this last result by proving the stability of the A_{FB} also against higher-order effects entering the hard scattering, in the form of the leading resummed QCD perturbative corrections. Indeed, since it is most often the case that A_{FB} ought to be combined with cross section (σ) measurements
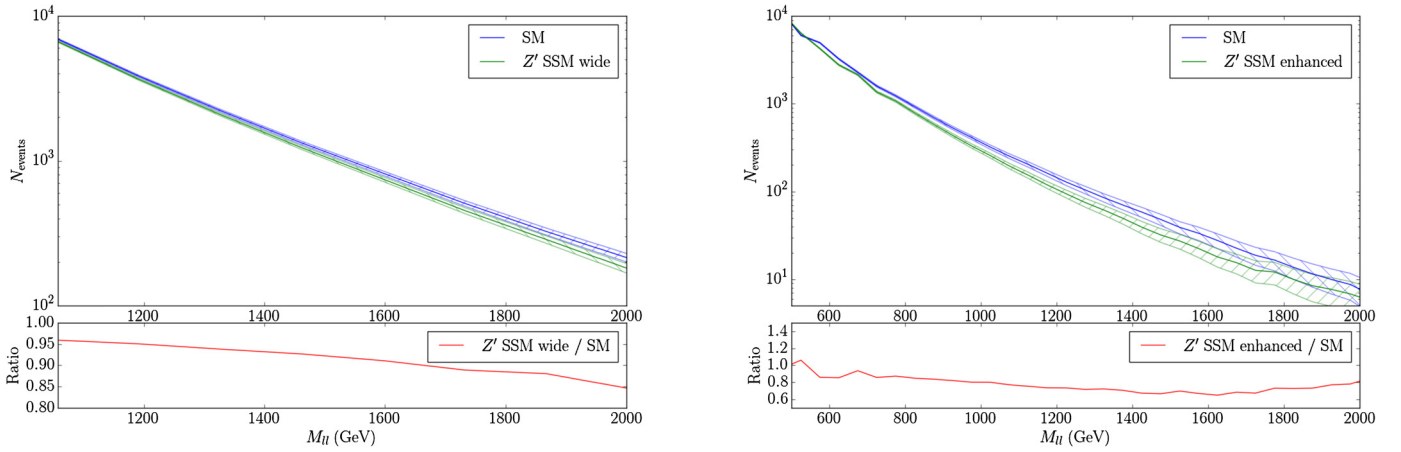
Fig. 5. Zoom-in of the di-lepton spectrum (calculated at NNLL) in the low invariant mass range end for (a) SSM wide scenario with luminosity of $L = 3000$ fb^{-1} and (b) SSM enhanced scenario with a luminosity of $L = 300$ fb^{-1}, both compared to the SM. The statistical error bands are shown. The ratios of BSM/SM are given in the sub-plots.

in order to both achieve Z' discovery and successfully diagnose its properties, we have extended the treatment of such higher-order QCD effects also to the case of differential σ observables. Crucially, this ought to be done not only for di-lepton quantities, but also for single lepton ones, in order to ensure that the acceptance region of the detector is not returning different efficiencies in the presence of a wide Z' (or these can be corrected for), with respect to the SM case. Here, we have studied all this using two benchmark scenarios, so-called 'SSM wide' and 'SSM enhanced', wherein the Z' is always sufficiently wide that sensitivity to it, above and beyond the SM yield, may first emerge in the low-mass tail of the di-lepton mass distribution, rather than the peak region, no matter its shape (being indeed more BW-like in the former than in the latter case). As the potential observation of such phenomenological effects is more dependent on experimental statistical than systematic errors, we have constructed these two scenarios in such a way that one (SSM enhanced) may be accessible at Run 3 luminosities while the other (SSM wide) may be so only with HL-LHC data samples. Finally, we have verified that the residual theoretical systematic error associated with the NNLL accuracy of our results is always much smaller in comparison to the experimental ones. In short, at the LHC, wide Z' scenarios may, on the one hand, no longer be elusive, thanks to a combination of σ and A_{FB} measurements, and, on the other hand, be separable from one another, thanks to the stability of the distributions enabling such a separation against the dominant higher-order QCD effects.

Acknowledgements

References

[1] P. Langacker, Rev. Mod. Phys. 81 (2009) 1199.
[2] A. Belyaev, R. Foadi, M.T. Frandsen, M. Jarvinen, F. Sannino, A. Pukhov, Phys. Rev. D 79 (2009) 035006, arXiv:0809.0793 [hep-ph].
[3] D. Barducci, A. Belyaev, S. De Curtis, S. Moretti, G.M. Pruna, J. High Energy Phys. 1304 (2013) 152, arXiv:1210.2927 [hep-ph].
[4] E. Accomando, D. Barducci, S. De Curtis, J. Fiaschi, S. Moretti, C. Shepherd-Themistocleous, PoS DIS 2015 (2015) 105, arXiv:1507.04245 [hep-ph].
[5] K. Agashe, R. Contino, A. Pomarol, Nucl. Phys. B 719 (2005) 165, arXiv:hep-ph/0412089.
[6] S. De Curtis, M. Redi, A. Tesi, J. High Energy Phys. 1204 (2012) 042, arXiv:1110.1613 [hep-ph].
[7] Y.G. Kim, K.Y. Lee, Phys. Rev. D 90 (2014) 117702, arXiv:1405.7762 [hep-ph].
[8] E. Malkawi, C.P. Yuan, Phys. Rev. D 61 (2000) 015007, arXiv:hep-ph/9906215.
[9] L. Basso, K. Mimasu, S. Moretti, J. High Energy Phys. 1211 (2012) 060, arXiv:1208.0019 [hep-ph].
[10] L. Basso, K. Mimasu, S. Moretti, J. High Energy Phys. 1209 (2012) 024, arXiv:1203.2542 [hep-ph].
[11] D. Barducci, S. De Curtis, K. Mimasu, S. Moretti, Phys. Rev. D 88 (2013) 074024, arXiv:1212.5948 [hep-ph].
[12] E. Accomando, K. Mimasu, S. Moretti, J. High Energy Phys. 1307 (2013) 154, arXiv:1304.4494 [hep-ph].
[13] L. Cerrito, D. Millar, S. Moretti, F. Spanò, PoS LHCP 2016 (2016) 239, arXiv:1610.04074 [hep-ph].
[14] L. Cerrito, D. Millar, S. Moretti, F. Spanò, arXiv:1612.03111 [hep-ph].
[15] E. Accomando, A. Belyaev, J. Fiaschi, K. Mimasu, S. Moretti, C.H. Shepherd-Themistocleous, PoS DIS 2015 (2015) 097.
[16] E. Accomando, A. Belyaev, J. Fiaschi, K. Mimasu, S. Moretti, C. Shepherd-Themistocleous, J. High Energy Phys. 1601 (2016) 127, arXiv:1503.02672 [hep-ph].
[17] E. Accomando, A. Belyaev, J. Fiaschi, K. Mimasu, S. Moretti, C. Shepherd-Themistocleous, Nuovo Cimento C 38 (2016) 153, arXiv:1504.03168 [hep-ph].
[18] J. Fiaschi, E. Accomando, A. Belyaev, K. Mimasu, S. Moretti, C.H. Shepherd-Themistocleous, PoS EPS -HEP2015 (2015) 176, arXiv:1510.05892 [hep-ph].
[19] E. Accomando, D. Barducci, S. De Curtis, J. Fiaschi, S. Moretti, C.H. Shepherd-Themistocleous, J. High Energy Phys. 1607 (2016) 068, arXiv:1602.05438 [hep-ph].
[20] E. Accomando, J. Fiaschi, S. Moretti, C.H. Shepherd-Themistocleous, Phys. Rev. D 96 (2017) 075019, arXiv:1703.04360 [hep-ph].
[21] E. Accomando, J. Fiaschi, F. Hautmann, S. Moretti, Phys. Rev. D 98 (2018) 013003, arXiv:1712.06318 [hep-ph].
[22] J. Fiaschi, E. Accomando, F. Hautmann, M. Klasen, S. Moretti, arXiv:1805.00842 [hep-ph].
[23] E. Accomando, J. Fiaschi, F. Hautmann, S. Moretti, Eur. Phys. J. C 78 (2018) 663, arXiv:1805.09239 [hep-ph], Erratum: Eur. Phys. J. C 79 (2019) 453.
[24] J. Fiaschi, E. Accomando, F. Hautmann, S. Moretti, arXiv:1906.11793 [hep-ph].
[25] E. Accomando, et al., J. High Energy Phys. 1910 (2019) 176, arXiv:1907.07727 [hep-ph].
[26] H. Abdolmaleki, et al., arXiv:1907.08301 [hep-ph].
[27] Y.L. Dokshitzer, D. Diakonov, S. Troian, Phys. Rep. 58 (1980) 269.
[28] G. Parisi, R. Petronzio, Nucl. Phys. B 154 (1979) 427.
[29] G. Curci, M. Greco, Y. Srivastava, Nucl. Phys. B 159 (1979) 451.
[30] J.C. Collins, D.E. Soper, Nucl. Phys. B 193 (1981) 381, Erratum: Nucl. Phys. B 213 (1983) 545.
[31] J. Kodaira, L. Trentadue, Phys. Lett. B 112 (1982) 66.
[32] J.C. Collins, D.E. Soper, G.F. Sterman, Nucl. Phys. B 250 (1985) 199.
[33] S. Catani, E. D'Emilio, L. Trentadue, Phys. Lett. B 211 (1988) 335.
[34] D. de Florian, M. Grazzini, Phys. Rev. Lett. 85 (2000) 4678, arXiv:hep-ph/0008152.
[35] S. Catani, L. Cieri, D. de Florian, G. Ferrera, M. Grazzini, Nucl. Phys. B 881 (2014) 414, arXiv:1311.1654 [hep-ph].
[36] S. Catani, M. Grazzini, Nucl. Phys. B 845 (2011) 297, arXiv:1011.3918 [hep-ph].

[37] G. Bozzi, S. Catani, G. Ferrera, D. de Florian, M. Grazzini, Phys. Lett. B 696 (2011) 207, arXiv:1007.2351 [hep-ph].

[38] S. Catani, D. de Florian, G. Ferrera, M. Grazzini, J. High Energy Phys. 1512 (2015) 047, arXiv:1507.06937 [hep-ph].

[39] S. Camarda, et al., arXiv:1910.07049 [hep-ph].

[40] F. Coradeschi, T. Cridge, Comput. Phys. Commun. 238 (2019) 262, arXiv:1711.02083 [hep-ph].

[41] F. Hautmann, H. Jung, A. Lelek, V. Radescu, R. Zlebcik, Phys. Lett. B 772 (2017) 446, arXiv:1704.01757 [hep-ph].

[42] F. Hautmann, H. Jung, A. Lelek, V. Radescu, R. Zlebcik, J. High Energy Phys. 1801 (2018) 070, arXiv:1708.03279 [hep-ph].

[43] A. Bermudez Martinez, et al., Phys. Rev. D 99 (2019) 074008, arXiv:1804.11152 [hep-ph].

[44] A. Bermudez Martinez, et al., Phys. Rev. D 100 (2019) 074027, arXiv:1906.00919 [hep-ph].

[45] W. Bizon, et al., J. High Energy Phys. 1812 (2018) 132, arXiv:1805.05916 [hep-ph].

[46] W. Bizon, et al., Eur. Phys. J. C 79 (2019) 868, arXiv:1905.05171 [hep-ph].

[47] I. Scimemi, A. Vladimirov, Eur. Phys. J. C 78 (2) (2018) 89, arXiv:1706.01473 [hep-ph].

[48] I. Scimemi, A. Vladimirov, J. High Energy Phys. 1808 (2018) 003, arXiv:1803.11089 [hep-ph].

[49] M.A. Ebert, F.J. Tackmann, J. High Energy Phys. 1702 (2017) 110, arXiv:1611.08610 [hep-ph].

[50] M.A. Ebert, J.K.L. Michel, F.J. Tackmann, J. High Energy Phys. 1705 (2017) 088, arXiv:1702.00794 [hep-ph].

[51] G. Billis, M.A. Ebert, J.K.L. Michel, F.J. Tackmann, arXiv:1909.00811 [hep-ph].

[52] T. Becher, M. Neubert, D. Wilhelm, J. High Energy Phys. 1202 (2012) 124, arXiv:1109.6027 [hep-ph].

[53] T. Becher, M. Neubert, D. Wilhelm, J. High Energy Phys. 1305 (2013) 110, arXiv:1212.2621 [hep-ph].

[54] F. Landry, R. Brock, P.M. Nadolsky, C.P. Yuan, Phys. Rev. D 67 (2003) 073016, arXiv:hep-ph/0212159.

[55] A.V. Konychev, P.M. Nadolsky, Phys. Lett. B 633 (2006) 710, arXiv:hep-ph/0506225.

[56] https://twiki.cern.ch/twiki/bin/view/LHCPhysics/LHCEW.

[57] G. Bozzi, in: A. Apyan, D. Froidevaux, F. Piccinini (Eds.), LHC Electroweak Working Group Meeting, CERN, July 2019, https://indico.cern.ch/event/829225/.

[58] G. Altarelli, B. Mele, M. Ruiz-Altaba, Z. Phys. C 45 (1989) 109, Erratum: Z. Phys. C 47 (1990) 676.

[59] E. Accomando, A. Belyaev, L. Fedeli, S.F. King, C. Shepherd-Themistocleous, Phys. Rev. D 83 (2011) 075012, arXiv:1010.6058 [hep-ph].

[60] G. Aad, et al., ATLAS Collaboration, Phys. Lett. B 796 (2019) 68, arXiv:1903.06248 [hep-ex].

[61] A.M. Sirunyan, et al., CMS Collaboration, J. High Energy Phys. 1806 (2018) 120, arXiv:1803.06292 [hep-ex].

[62] CMS Collaboration [CMS Collaboration], CMS-PAS-EXO-18-006.

[63] E. Accomando, D. Becciolini, A. Belyaev, S. Moretti, C. Shepherd-Themistocleous, J. High Energy Phys. 1310 (2013) 153, arXiv:1304.6700 [hep-ph].

[64] S. Dulat, et al., Phys. Rev. D 93 (2016) 033006, arXiv:1506.07443 [hep-ph].

[65] R. Hamberg, W.L. van Neerven, T. Matsuura, Nucl. Phys. B 359 (1991) 343, Erratum: Nucl. Phys. B 644 (2002) 403.

[66] R.V. Harlander, W.B. Kilgore, Phys. Rev. Lett. 88 (2002) 201801, arXiv:hep-ph/0201206.

[67] V. Khachatryan, et al., CMS Collaboration, J. High Energy Phys. 1504 (2015) 025, arXiv:1412.6302 [hep-ex].

[68] F. Coradeschi, T. Cridge, in preparation.

[69] N.K. Nielsen, Nucl. Phys. B 101 (1975) 173.

[70] W. Konetschny, W. Kummer, Nucl. Phys. B 100 (1975) 106.

[71] H. Kluberg-Stern, J.B. Zuber, Phys. Rev. D 12 (1975) 467.

[72] M. Consoli, A. Sirlin, in: J. Ellis, R.d. Peccei (Eds.), Physics At LEP, CERN 86-02, Vol. 1, 1986, pp. 63–89.

[73] P.A. Grassi, B.A. Kniehl, A. Sirlin, Phys. Rev. D 65 (2002) 085001, arXiv:hep-ph/0109228.

[74] G. Altarelli, R.H.P. Kleiss, C. Verzegnassi, CERN-89-08-V-1, https://cds.cern.ch/record/116932, 1989.